RSC Advances

ROYAL SOCIETY OF CHEMISTRY

www.rsc.org/advances

Journal Name

RSCPublishing

ARTICLE

Engineering the epoxide hydrolase from *Agromyces mediolanus* for enhanced enantioselectivity and activity in the kinetic resolution of racemic epichlorohydrin

Cite this: DOI: 10.1039/xoxxoooooox

Received ooth January 2012,
Accepted ooth January 2012

DOI: 10.1039/xoxxoooooox

www.rsc.org/

Feng Xue[a,b], Zhi-Qiang Liu[a,b], Nan-Wei Wan[a,b], Hang-Qin Zhu[a,b], Yu-Guo Zheng[a,b]*

The biocatalytic production of enantiopure epichlorohydrin (ECH) has been steadily drawing more attentions. For industrial application, it is important to obtain an epoxide hydrolase (EH) that possesses the desired enantioselectivity. Site-saturation and site-directed mutagenesis of positions Ser207, Asn240 and Trp182 were used to generate variants of EH from *Agromyces mediolanus* ZJB120203 with enhanced enantioselectivity for kinetic resolution of racemic ECH. The best variant VDF (W182F/S207V/N240D) has 7-fold enhanced enantioselectivity toward racemic ECH, with the enantiomeric ratio value (*E* value) preferring (*R*)-ECH increased from 12.9 of wild-type to 90.0, as well as 1.7-fold improved activity. Furthermore, we successfully applied the created recombinant *Escherichia coli* whole cells expressing variant VDF in the kinetic resolution of racemic ECH. Enantiopure (*S*)-ECH could be obtained with an enantiopurity of > 99% *ee* and a yield of 40.5% from 450 mM racemic ECH, which is better than other reported EHs. These results demonstrated that the EH obtained in this study could be applied into the efficient resolution of the racemic ECH.

Introduction

Epoxide hydrolases (EHs; EC 3.3.2.3), ubiquitous enzymes found in mammals, insects, plants, and microorganisms, catalyze the hydrolysis of epoxides to corresponding vicinal diols with the addition of a water molecule.[1, 2] Most EHs for which sequence information is presently available are members of the α/β-hydrolase fold family and share a main domain consisting of a central β sheet surrounded by α helices, with a variable cap domain sitting on top.[2, 3] The catalytic triad is formed of a nucleophile (Asp), which attacks the epoxide and forms a covalent ester-intermediate, a catalytic histidine and a carboxylic acid (Asp or Glu) which subsequently activate a water molecule and hydrolyze the ester bond to release the product.[4, 5]

In the past 20 years, EHs have been explored for the preparation of optically active epoxides and diols. The most common application of EHs is the preparation of optically pure epoxides by enantioselective hydrolysis of a racemic epoxide.[6] Enantiopure epichlorohydrin (ECH) is a valuable epoxide intermediate for producing optically active pharmaceuticals. ECH has been used for the synthesis of β-blockers, L-carnitine, ferroelectric liquid crystals, atorvastatin.[7, 8] Several enantioselective EHs have been tested in kinetic resolutions to obtain an enantiopure ECH. However, the yield of the remaining ECH and the enantiopurity of the diol are often not very high due to the low enantioselectivity of the EH.[9-11] Therefore, it is desirable to improve the enantioselectivity of EHs.

It is reported that site-directed mutagenesis, saturation mutagenesis, error-prone polymerase chain reaction and DNA shuffling, have been applied to enhance the activity and enantioselectivity of EHs.[12-16] Through high throughput screening method, EH mutants with improve functions have been obtained, which shows a good prospect for EHs in biotechnological applications. [12, 13, 15-18]

In our previous study, a novel EH from *Agromyces mediolanus* ZJB120203 (AmEH) was cloned and expressed in *E. coli*. The kinetic mechanism of AmEH was solved in detail for both enantiomers of ECH, and wild-type (WT) AmEH was determined to be moderately enantioselective toward (*R*)-ECH (Fig. S1†).[5] The variants constructed in this study were evaluated for altered enantioselectivity and activity toward racemic ECH. Further, saturation mutagenesis was used to engineer AmEH with altered enantioselectivity and enzymatic activity toward racemic ECH. The residues, especially those having a near-reaching effect on substrate binding that are reliably predicted by rational design, have been identified. Production of optical pure (*S*)-ECH was also detailedly studied and optimized.

Results and discussion

Construction and screening of mutant libraries of AmEH

In order to choose appropriate randomization sites, we performed homologous modelling of AmEH using the EH structure (PDB accession no. 4i19) as template and further induced fit docking of (*R*)-ECH and (*S*)-ECH into the obtained model. It is well recognized that residues adjacent to the substrate play critical roles in catalytic activity and enantioselectivity, thus will commonly act as the target sites for rational design.[19] The HotSpot Wizard could give

predictions to hot spots (The amino acid residues that mediate the substrate binding, transition-state stabilization or product release are frequently selected as 'hot spots'.) in enzymes based on structural, functional and evolutionary information obtained from different databases.[20] In the case of AmEH, HotSpot Wizard lists annotated residues ordered by estimated mutability. Based on different considerations, Trp182, Ser207, Ser233, Asn240, Arg313, Phe318 and Arg338 were chosen for mutagenesis and catalytic property analysis (Fig. 1).

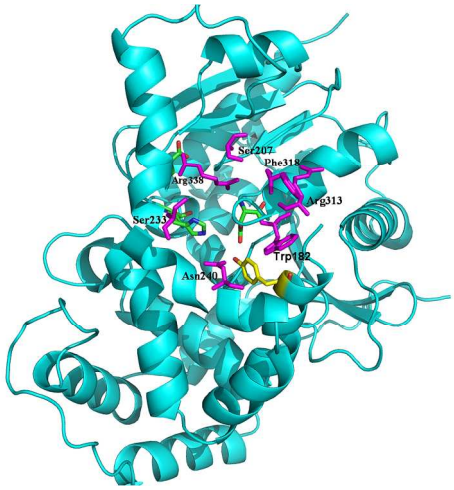

Fig.1 Sites for mutant were chosen as described in the text and color coded as magenta.

7 libraries were generated using saturation mutagenesis, ideally each containing all possible amino acid substitutions at one of these positions. These mutant libraries were screened for hydrolysis activity towards ECH by using 4-(4-nitrobenzyl)pyridine (NBP), which reacts with terminal epoxides to form a blue adduct that can be qualitatively analysed (Fig. 2). After screening 2000 clones, approximately 50% showed appreciable activity as revealed by the pretest, and subsequently applied automated GC in order to obtain the respective conversion and *ee* values. The cell free extracts of WT AmEH and variants were purified by one-step nickel affinity chromatography on Ni-NTA resin. After SDS-PAGE, it was found that there was no difference in the molecular mass (about 43 kDa) between the WT and mutant AmEH, which was similar to the previous report (Fig. S2†).[5]

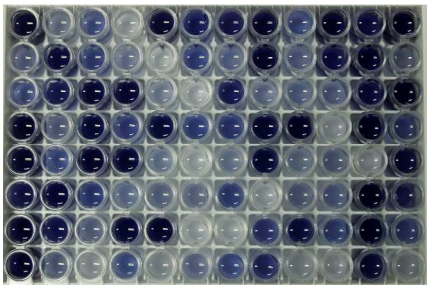

Fig. 2 Activity screening of the site-saturation library for ECH in 96-well plates using NBP assay

For most of the mutants, the yields of (*S*)-ECH were declined, indicated that their enantioselectivities were decreased towards racemic ECH. No positive mutant with improved enantioselectivity was isolated at position Arg313, Arg338, Ser233 and Phe318. A series of variants from the libraries of the other three sites (Ser207, Trp182 and Asn240) showed higher enantioselectivity enhancement over wild-type enzyme (data not shown). Among the mutants, three variants with the highest enantioselectivities at each position, S207V, W182F and N240D, were selected and subsequently shown to have not only increased total activity, but also increased (*R*)-enantioselectivity (Table 1). The introduction of Val instead of a Ser at position 207 raised the *E*-value from 12.9 to 20.3. The introduction of Asp instead of a Asn at position 240 raised the *E*-value from 12.9 to 21.4.

In EHs, the residue next to the active site nucleophilic amino acid is not strictly conserved, but it is often a tryptophan, such as the Trp182 in AmEH.[21, 22] The corresponding residue was Phe108 in EH from *Agrobacterium radiobacter* AD1, which has been investigated and confirmed by saturation mutagenesis. Mutants of EH from *A. radiobacter* AD1 at this position have great impacts on the activity and enantioselectivity. Mutant F108W of EH from *A. radiobacter* AD1 had decreased enantioselectivities and activities for all the test aromatic substrates, whereas for the two aliphatic epoxides, the activities were lower than wild type.[17] The mutation of Trp182 of AmEH had improved the enantioselectivity and activity for ECH as compared to the WT. The changes in both enantioselectivity and activity as a result of mutations at this position provide further evidence that the side chain of this conserved residue is involved in substrate binding. The conservative tyrosine residues were proposed to stabilize the transition state towards the formation of the intermediate by protonation of the leaving oxygen group. Based on the previous report,[23] Asn240 flanking the Tyr239 was also proposed as potential hot spots for enhancing activity and enantioselectivity. The mutagenesis studies have revealed that N240D had higher activity (2.4-fold) than the WT, while its *E*-value raised from 12.9 to 21.4. Based on the structure analysis, it is found that another residue Ser207 was position in a loop, and closely located to the catalytic residues, approximately on a distance of 8.3 Å. Mutation of Ser207 therefore ought to have some impact on the catalytic efficiency of AmEH. For ECH, the mutant S207V had a higher enantioselectivity and activity, which showed that Ser207 plays a role in the AmEH-catalyzed hydrolysis of ECH. These studies showed that residues Trp182, Ser207 and Asn240 were enantioselectivity "hot spots" with several mutants affording product (*S*)-ECH with high *ee*, and residue Asn240 exerted a greater effect on the enzyme activity than residues Ser207 and Trp182.

Combination of mutations can have additive effects in the case of enantioselectivity (Table 1). For the AmEH mutants, two and three pronounced additive effects on enantioselectivity were also found, except the variant W182F/N240D, which had decreased the enantioselectivity and activity for ECH (data not shown). Several variants (W182F/S207V, S207V/N240D and W182F/S207V/N240D) isolated from the second and third-generation library, VD and VDF, are particularly efficient in the kinetic resolution of ECH. VD contains two active-site substitutions, S207V and N240D, VDF also contains S207V and N240D, but in combination with W182F. Variants VD increased the enantioselectivity from 12.9 to 48.1 towards racemic ECH. However, VDF was most distinct, with the *E* value increasing from 12.9 for the wild-type enzyme to 90.0, a 7-fold enhancement, which is the highest enantioselectivity described for ECH so far. In addition, VDF also demonstrated a 1.7-fold improvement compared with the WT AmEH in specific activity. The significant improvement in enantiomeric purity and the enhanced catalytic rate made VDF an AmEH variant of considerable interest for preparing enantiomerically pure (*S*)-ECH.

Table 1 Specific activities and enantioselectivities of wild-type AmEH and variants toward racemic ECH

Enzyme	Racemic ECH		Enantioselectivity	
	Specific activity (U/mg)	Fold	*E*-value[a]	Fold
Wild-type	24.6	1.0	12.9	1.0
W182F	26.1	1.1	16.9	1.3
S207V	38.9	1.6	20.3	1.6
N240D	59.7	2.4	21.4	1.7
W182F/S207V	30.1	1.2	28.5	2.2
VD	69.0	2.8	48.1	3.7
VDF	42.6	1.7	90.0	7.0

[a] *E* values are calculated from the k_{cat}/K_m values for the separate enantiomers.

Kinetics parameters analysis of selected mutants

Enhancing the enantioselectivity of a kinetic resolution can be carried out by increasing the reaction rate of one enantiomer, or by decreasing the rate of the mirror-image compound.[12] To understand the basis of the observed changes in enantioselectivity, the steady-state kinetic parameters of the mutants were determined for ECH using enantiopure as substrate. Kinetic parameters (K_m, V_{max}, k_{cat} and k_{cat}/K_m) of AmEH and variants toward (*R*)-ECH and (*S*)-ECH were determined and summarized in Table 2. The results showed that the overall catalytic efficiencies (k_{cat}/K_m) of mutant AmEHs were lower than WT enzymes for (*S*)-ECH, while for mutant AmEH, the k_{cat}/K_m values were higher than the WT enzyme for (*R*)-ECH. VDF gave a k_{cat}/K_m value for the (*R*)-enantiomer that was 2.0-fold greater than that of the WT. However, the k_{cat}/K_m of VDF for (*S*)-ECH was reduced to about one quarter of the WT. The changes in kinetic parameters for VDF led to a significant enhancement in the *E*-value. For mutant VD there is also a significant increase in k_{cat}/K_m on (*R*)-ECH and decrease in k_{cat}/K_m on (*S*)-ECH. For the mutant N240D the increase in enantioselectivity is mainly due to an increased k_{cat} for its preferred substrate, (*R*)-enantiomer.

Moreover, the mutations also caused the changes in the V_{max} values. The N240D mutant had a V_{max} value for (*R*)-ECH that was approximately 2.5 times that of the WT, whereas it had a lower V_{max} value for (*S*)-ECH. These results clearly support the hypothesis concerning the two roles of Asp240, which is enhancement of reactivity in (*R*)-ECH and suppression of the reactivity in (*S*)-ECH. Furthermore, the VD double mutant had a V_{max} value for (*R*)-ECH that approximately 1.2 times that of the N240D mutant.

Table 2 Kinetic analysis of the selected mutants of AmEH towards enantiopure ECH

Enzyme	*S*-ECH				*R*-ECH			
	K_m (mM)	V_{max} ($\mu molmin^{-1}mg^{-1}$)	k_{cat} (s^{-1})	k_{cat}/K_m ($mM^{-1}s^{-1}$)	K_m (mM)	V_{max} ($\mu molmin^{-1}mg^{-1}$)	k_{cat} (s^{-1})	k_{cat}/K_m ($mM^{-1}s^{-1}$)
WT	161.4	7.9	5.7	3.5×10^{-2}	56.6	35.6	25.7	4.5×10^{-1}
W182F	130.7	5.9	4.2	3.2×10^{-2}	48.3	36.2	26.1	5.4×10^{-1}
S207V	108.8	4.8	3.5	3.2×10^{-2}	62.6	56.4	40.7	6.5×10^{-1}
N240D	141.8	6.8	4.9	3.5×10^{-2}	87.3	90.3	65.2	7.5×10^{-1}
W182F/ S207V	137.1	3.8	2.7	2.0×10^{-2}	52.1	41.1	29.7	5.7×10^{-1}
VD	134.0	2.9	2.1	1.6×10^{-2}	98.7	105.3	76.0	7.7×10^{-1}
VDF	105.1	1.5	1.1	1.0×10^{-2}	48.8	60.5	43.7	9.0×10^{-1}

Homology structural modeling and substrate docking

The three-dimensional coordinates of the AmEH variants with the most significant changes in ECH hydrolysis, N240D, VD and VDF, were constructed, and molecular docking was further carried out and tried to deeply understand the interactions between the enantiomers of ECH and the amino acid residues in the AmEH active cavity (Fig. 3, Table S2†). Docking of the ECH into the active sites of the various mutants and wild type suggest the reshaping of the binding pocket. The catalytic efficacy of the enzyme is dependent on how often the nucleophile and electrophile are present in near attack conformations (NACs). The through-space distance, *d*, between the attacking O-atom of Asp181 and the epoxide C-atom was thought to be of particular importance, and the angle from the Asp181 oxygen *via* the attacked epoxide carbon to the epoxide oxygen (α_1) and the Asp181 oxygen *via* the attacked epoxide carbon to the other epoxide carbon (α_2) were also considered.[24]

As Table S2† shown, the favored enantiomers have relatively shorter distance (*d* value) and larger angles (α_1 and α_2 value), corresponding to NACs or more generally to productive positions, as expected. The differences in the modeled distance, $\triangle d$, for the (*R*)-ECH and (*S*)-ECH were well consistent with the measured *E* values.[7,25] In the WT AmEH, the $\triangle d$ value is expected to be only 0.3 Å, with the preferred (*R*)-ECH slightly closer to the attacking Asp181.[5] In the mutant VD, the $\triangle d$ value was increased to 0.9 Å. For the preferred (*R*)-ECH, the value for *d* was reduced to 3.2 Å, which may be responsible for the about 2.8-fold increase in the activity for this variant. However, for the disfavor (*S*)-ECH, the value *d* was increased to 4.1 Å. In the case of the highly enantioselective VDF, the result is remarkably different; and $\triangle d$ has increased to 1.1 Å. For the preferred (*R*)-ECH, the value for *d* does not change evidently (*d* =3.3 Å), but the activated (*S*)-ECH is positioned much further away (*d*=4.4 Å), which disfavors ring opening nucleophilic attack. Additionally, the calculation results shown that there was a bigger difference than WT AmEH in angle values between (*R*)-ECH (142.0° and 136.8°) and (*S*)-ECH (55.2° and 64.7°), which leads to the best mutant VDF was more active on (*R*)-ECH. These results suggested that structural changes in the binding pocket imposed by the evolutionary process are predicted to make it much more difficult for the disfavored (*S*)-ECH to experience activation by the Tyr308 and at the same time to be positioned close enough to Asp181 for rapid nucleophilic attack.[12]

a

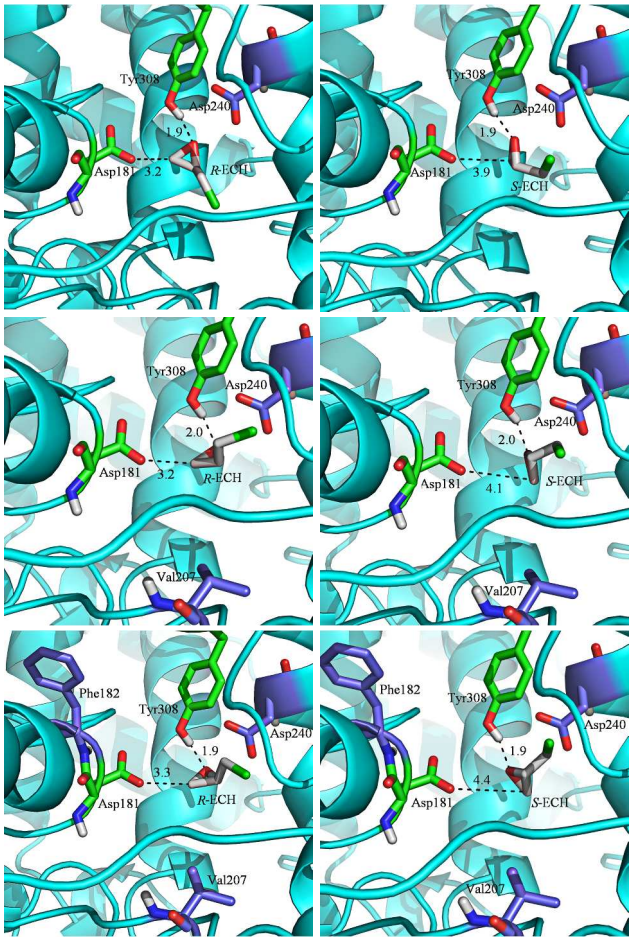

Fig. 3 Docking of (*R*)-ECH and (*S*)-ECH to the binding pocket of mutant AmEHs. (a) Variant N240D docked with (*R*)-ECH and (*S*)-ECH; (b) Variant VD docked with (*R*)-ECH and (*S*)-ECH; (c) Variant VDF docked with (*R*)-ECH and (*S*)-ECH.

Biocatalytic synthesis of chiral ECH using recombinant cells of variant VDF

To test the potential applications of the mutant in enzymatic hydrolysis of ECH, the recombinant *E. coli* (4.5 g dcw/L) used as biocatalyst was incubated with racemic ECH at the substrate concentrations of 75 and 150 mM. The time-course of the kinetic resolution of racemic ECH is shown in Fig. S3†. As a result, the enantiopure (*S*)-ECH with more than 99% *ee* was obtained from 75 mM and 150 mM racemic ECH with the yield from 45.8% to 44.1% (theoretical, 50%). Considering the industrial applicability, a low concentration of substrate may be a major restriction for the enzymatic reaction. Thus, we verified if the reaction could go beyond 150 mM ECH with keeping the optical yield and enantioselectivity as the amount of enzyme increased. As shown in Fig. S3†, 8.5 and 13.5 g dcw/L recombinant *E. coli* were incubated with racemic ECH ranging from 150 to 300 mM at 30 °C and pH 8.0. As a result, it was found that enantiopure (*S*)-ECH with a high optical purity (*ee* > 99%) was readily obtained from 150 to 300 mM racemic ECH within 80 min, and more AmEH expenditure in the reaction could help to shorten the reaction time without significantly affecting optical yield and enantioselecticity. When kinetic resolution was conducted by the recombinant *E. coli* at ECH concentration of 450 mM, chiral (*S*)-ECH with an *ee* higher than

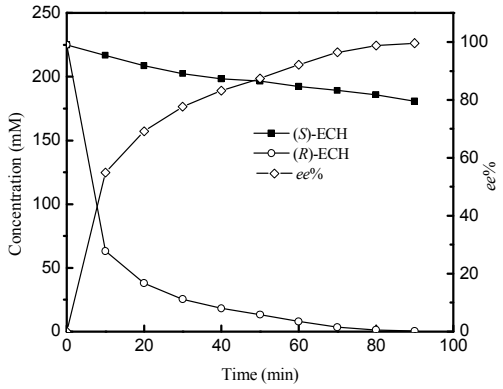

Fig. 4 Enantioselective hydrolysis of racemic ECH by the recombinant *E. coli* variant VDF. The reaction was performed at 30 °C in 200 mM sodium phosphate buffer (pH 8.0), 450 mM ECH and 13.5 g dcw/L recombinant *E. coli*. Samples were removed at time intervals, the ECH concentration and the optical purity of the (*S*)-ECH were determined by chiral GC.

99% was obtained as 40.5% yield (theoretical, 50%) at 90 min (Fig. 4). In the best known examples, EH from *Novosphingobium aromaticivorans* has been cloned and applied into resolution of (*R,S*)-ECH (250 mM) to provide (*S*)-ECH with only 17.3% yield and more than 99% *ee* (Table 3).[11] In the last decades, the use of EHs in the kinetic resolution of racemic ECH for synthesis of chiral ECH, is still hindered by the insufficient enantioselectivity of existing EHs [5, 7, 9, 26], and ECH is a very unstable epoxide in aqueous buffer.[10] These two disadvantages led to a poor yield of enantiopure ECH from the kinetic resolution that occurred in the aqueous phase. The variant VDF catalyzed the enantioselective hydrolysis of racemic ECH to give (*S*)-ECH with an enantiomeric ratio (*E*) of 90.0 in aqueous buffer, better than any reported EHs, which making it very competitive and promising for practical applications in production of (*S*)-ECH. However, when the concentration reached 500 mM, the optical purity of (*S*)-ECH was only 90.1%, even when the reaction time was prolonged to 200 min. When the variant VD (S207V/N240D) was used in the production of (*S*)-ECH by kinetic resolution of racemic ECH, the *ee* of (*S*)-ECH was able to reach 99% at high concentration of 750 mM racemic ECH, although the yield was not excellent (about 21.3%). This result may be due to the mutant VDF has higher enantioselectivity, but lower activity than mutant VD. To our knowledge, the substrate and product inhibition was always the limitation of large-scale applications in many biotransformation reactions.[27, 28] This may be ascribed to the enzyme inactivation caused by a high concentration of the substrate and product. This type of inhibition has been reported in the asymmetric reduction of ECH and can be overcome by utilizing substrate fed-batch strategy and an aqueous-organic is solvent two-phase system.[29, 30] EHs should be tuned for better operational stability for the application in non-natural reaction conditions. It is of interest to improve the stability of EHs in organic solvents and to prevent the interfacial deactivation of EHs in aqueous/organic two phase system by molecular engineering of EHs.

Experimental section

Materials, bacterial strains and plasmids

(*R,S*)-ECH, (*R*)-ECH, (*S*)-ECH and NBP were purchased from Sigma-Aldrich (St. Louis, MO, USA). All other chemicals used were of analytical grade and are commercially available.

Journal Name RSCPublishing

ARTICLE

Table 3 The comparison of kinetic resolution of known EHs toward racemic ECH

EH source	ECH conc (mM)	Temperature (°C)	pH	*ee*(%)	Reaction medium	Final yield[a] (%)	Reference
Aspergillus niger	60	27	7.5	100/(*S*)	organic solvents	20.0	10
Novosphingobium. aromaticivorans	50	30	8.0	>99/(*S*)	aqueous buffers	20.7	11
Novosphingobium. aromaticivorans	250	30	8.0	>99/(*S*)	aqueous buffers	17.3	11
Aspergillus niger	64	30	8.0	98/(*S*)	organic solvents	17.5	27
Agromyces mediolanus (AmEH)	64	30	8.0	>99/(*S*)	aqueous buffers	21.5	5
Mutant AmEH (W182F/S207V/ N240D)	75	30	8.0	>99/(*S*)	aqueous buffers	45.8	This study
	150	30	8.0	>99/(*S*)	aqueous buffers	44.1	This study
	300	30	8.0	>99/(*S*)	aqueous buffers	43.7	This study
	450	30	8.0	>99/(*S*)	aqueous buffers	40.5	This study

[a] The final yield of (*S*)-ECH was determined by GC.

PrimeSTAR HS DNA polymerase, restriction endonucleases, PCR reagents and the genomic extraction kit were purchased from Takara Biotechnology (Dalian, China) Co., Ltd. DNA sequencing was performed by Sangon Biotechnology (Shanghai, China) Co., Ltd. The DNA gel extraction, plasmid extraction and PCR product purification kits were purchased from Axygen Biotechnology (Hangzhou, China) Co., Ltd. *E. coli* BL21(DE3) and pET-28a(+) were used as the host strain and vector for expression experiments. The plasmid pET28a-AmEH with the gene encoding EH from *A. mediolanus* ZJB120203 was used as the template for saturation mutagenesis. The *E. coli* strains were grown at 37 °C in lysogeny broth (LB) medium (0.5% yeast extract, 1% tryptone and 1% NaCl), and supplemented with kanamycin (50 μg/ml).

Construction of saturation mutagenesis libraries

Gene libraries encoding all possible amino acids at positions 182, 207, 233, 240, 313, 318 and 338 of the AmEH gene in the pET28a-*ameh* (pET-28a hosting the gene encoding AmEH) were constructed by replacing the target condon with NNN (N=A/T/C/G in a 1:1:1:1 ratio) *via* polymerase chain reaction (PCR). The primers used for saturation mutagenesis at each site are listed in Table S1†. The mutagenesis PCR was performed with PrimeSTAR HS DNA polymerase using a program of 3 min at 98 °C followed by 27 cycles of 98 °C for 10 s, 55 °C for 15 s, 72 °C for 7 min and a final extension at 72 °C for 10 min. The restriction enzyme *Dpn* I was directly added to the PCR reaction tube to degrade the methylated template for 3 h at 37 °C. The mixture was transformated into *E. coli* BL21(DE3) and cultivated on the LB agar plate containing 50 μg/ml kanamycin. The transformants were confirmed by DNA sequencing using the T7 forward and reverse primer. From three positive mutants, a second round of site-directed mutagenesis was performed at the two other respective amino acid residues. The mutant with improved enzyme activity and enantioselectivity was obtained by site-directed mutagenesis and screening.

Protein expression and purification

The recombinant *E. coli* was cultivated at 37 °C and 200 rpm orbital shaking in 100 ml of LB broth containing 50 μg/ml kanamycin. After the cells reached an OD_{600} of 0.6, heterologous expression of the protein was induced fully with 0.1 mM isopropyl-β-D-thiogalactoside (IPTG) and the culture was continuously incubated at 28 °C for additional 10 h. The cells were harvested, disrupted by sonication using an ultrasonic processor UP200S (Hielscher, Teltow, Germany) and centrifuged for 15 min at 4 °C and 10,000 × *g*. The WT AmEH and mutant variants were purified by the AKTA™ explorer system (Amersham Biosciences Corp., Uppsala, Sweden) with a 16 mmD/100 mmL POROS MC 20 μm column (Applied Biosystems Co., USA). His-tagged enzyme was bound to the resin in equilibrating buffer (20 mM sodium phosphate buffer, pH 8.0, containing 0.5 M sodium chloride, and 20 mM imidazole). Unbound and weakly bound proteins were washed out. His-tagged enzyme was eluted by a buffer containing 500 mM imidazole.[31] The eluted protein was pooled and dialyzed overnight against 20 mM sodium phosphate buffer (pH 8.0) and then stored at 4 °C.[32] The protein concentration was quantified via the Bradford method using bovine serum albumin (Sigma-Aldrich, St. Louis, MO, USA) as the standard.[33] The molecular mass of the denatured protein was determined by 12% sodium dodecyl sulfate polyacrylamide gel electrophoresis (SDS-PAGE) as described by Laemmli.[34] The protein was stained with Coomassie brilliant blue G-250 (Aladdin, Shanghai, China).

Determination of kinetic properties

The kinetic analysis of the WT and AmEH variants for kinetic resolution of racemic ECH was performed by measuring their initial rates towards varied concentration of (*R*)-ECH and (*S*)-ECH, respectively. The maximum reaction rate V_{max} and Michaelis constant K_m were determined using Lineweaver-Burk plotting method based on the Michaelis-Menten equation: $1/v=K_m/V_{max}[S]+1/V_{max}$, where v is the initial velocity and [S] is the substrate concentration. The catalytic constant k_{cat} was deduced

using a molecular mass of 43 kDa. All parameters were calculated using the mean values from three independent experiments. The *E*-value, corresponding to the enantioselectivity of the enzyme, was derived from the ratio of k_{cat}/K_m of the separate enantiomers.

Activity screening

The constructed mutant libraries were screened for EH activity using a blue assay in a 96-well plate developed by Cedrone.[35] All colonies from the agar plate prepared in the earlier step were picked using a 10 µl micropipette tip and directly transferred into individual well in 96-well containing 1 ml of LB medium with kanamycin. The plates were incubated at 37 °C for 2 h, and induced with 0.1 mM IPTG for the heterologous expression of EH. The expression plates were incubated overnight at 28 °C on a shaker. After centrifuging for 20 min at 3,000 × *g*, the cell pellets were resuspended in 200 µl 50 mM phosphate buffer (pH 8.0). Aliquots (25 µl) of the supernatant were transferred to the new microtiter plates containing 25 µl of epoxide substrate solution (5 mM racemic ECH dissolved in 50 mM phosphate buffer). After incubation at 30 °C for 20 min, the reaction was stopped by addition of 25 µl of 100 mM 4-(4-nitrobenzyl) pyridine in a 80/20 v/v ethylene glycol/ethanol mixture. The reaction of NBP with ECH was run for 20 min at 80 °C and 50 µl ethanol and 25 µl 1 M K_2CO_3 were added. The K_2CO_3 interacts with the remaining ECH and a blue color was developed. The darker the blue color of the solution, the more ECH is left unconverted in the well, indicating inefficient mutant variants or absence of enzyme.

Activity assay and analytical methods

The standard assay was performed with racemic ECH and the recombinant EH mixed in 10 ml phosphate buffer (pH 8.0). The reaction mixture reaction was incubated at 30 °C, 150 rpm. After 5 min, 1.0 ml biotransformation sample was taken and centrifuged at 12,000 × g for 5 min and then 400 µl of biotransformation sample was extracted with 1 ml of ethyl acetate and centrifuged at 10,000 × g for 5 min. The organic layer was separated and dried with anhydrous sodium sulfate. The reaction mixture was analyzed by GC and chiral GC to determine the enzyme activity and *ee* value, respectively. The concentrations of the ECH was analyzed by using Agilent 7890A gas chromatograph (Agilent, Santa Clara, CA) with a capillary HP-5 column (0.35 mm × 30 m × 0.25 µl film thickness). Temperature program: 80 °C for 4 min, and then to 100 °C at 10 °C/min. Retention times: 4.7 min for racemic ECH, 5.8 min for 1-chlorohexane (internal standard). Enantioselectivity was determined by GC equipped with a chiral capillary BGB-175 column (0.25 mm × 30 m × 0.25 µl film thickness). Injector, detector and column temperatures are set as 220, 220 and 90 °C, respectively. The retention times of (*S*)-ECH and (*R*)-ECH were 4.7 and 4.9 min, respectively.[5] The *ee* was derived from the remaining epoxide of the two enantiomers [*ee* (%)=(*S*-*R*)/(*S*+*R*)×100]. One unit of EH activity was defined as the amount of enzyme required to convert 1 µmol ECH at 30 °C. Specific enzyme activities were defined as units per mg enzyme per min.

Biocatalytic synthesis of chiral ECH by the whole-cell biocatalyst

Enantioselective hydrolysis of racemic ECH was conducted in 50 ml screw-capped vials with the working volume of 10 ml. The cultured cells were suspended in a 200 mM sodium phosphate buffer (pH 8.0), and the kinetic resolution reactions were initiated with the addition of various concentration of racemic ECH at 30 °C in a shaking incubator (200 rpm). The reaction was then stopped by extraction twice with an equal volume of ethyl acetate. The progression of the enantioselective hydrolysis reaction was analyzed by the analysis of samples withdrawn periodically from the reaction mixtures.

Molecular modeling and analysis

The crystal structure of an EH from *Streptomyces carzinostaticus* (PDB accession no. 4i19), which was 36% identical to AmEH, was chosen as the template. The three-dimensional homology model of WT and AmEH mutants were generated by Modeller 9.12 in Discovery studio (DS) 2.1 (Accelrys Software, San Diego, USA) with loops refined sufficiently.[36, 37] Several models were obtained and validated by Procheck and Profile-3D. Finally, the best quality model was chosen for further calculations, molecular modeling, and docking studies by Autodock 4.0.[38] The visualization was performed with PyMOL program version 1.2r1 (http://www.pymol.org).

Conclusions

In summary, the enantioselectivity and activity of AmEH toward (*R*, *S*)-ECH were improved by a structure-based rational design approach. Successive rounds of saturation mutagenesis resulted in an increase in enantioselectivity from *E*=12.9 for the WT enzyme to *E*=90.0 for the best variant (W182F/S207V/N240D). Enantiopure (*S*)-ECH could be readily prepared with high enantiopurity more than 99% *ee* and yield of 40.5% by using the three-point mutant with 450 mM (*R*, *S*)-ECH as substrate. These results indicated that the engineered EH is a promising biocatalyst for kinetic resolution of racemic ECH and other substrates.

Acknowledgments

This work was financially supported by National Natural Science Foundation of China (No. 21176224), National High Technology Research and Development Program of China (No.2012AA022201B), 973 Program (No. 2011CB710806).

Notes and references

[a]Institute of Bioengineering, Zhejiang University of Technology, Hangzhou, Zhejiang 310014, P. R. China; Tel.:+86-571-88320630; Fax: +86-571-88320630 E-mail address: zhengyg@zjut.edu.cn;
[b]Engineering Research Center of Bioconversion and Biopurification of the Ministry of Education, Zhejiang University of Technology, Hangzhou, Zhejiang 310014, P. R. China

†Electronic Supplementary Information (ESI) available: [Result details]

1 M. Arand, A. Cronin, M. Adamska and F. Oesch, *Phase Ii Conjugation Enzymes and Transport Systems*, 2005, **400**, 569- 588.
2 Z. Q. Liu, Y. Li, Y. Y. Xu, L. F. Ping and Y. G. Zheng, *Appl. Microbiol. Biotechnol.*, 2007, **74**, 99-106.
3 M. Widersten, A. Gurell and D. Lindberg, *BBA-Gen Subjects*, 2010, **1800**, 316-326.
4 N. Bala and S. S. Chimni, *Tetrahedron-Asymmetr.*, 2010, **21**, 2879-2898.
5 F. Xue, Z. Q. Liu, S. P. Zou, N. W. Wan, W. Y. Zhu, Q. Zhu and Y. G. Zheng, *Process Biochem.*, 2014, **49**, 409-417.
6 M. Kotik, A. Archelas and R. Wohlgemuth, *Curr. Org. Chem.*, 2012, **16**, 451-482.
7 Z. Q. Liu, L. P. Zhang, F. Cheng, L. T. Ruan, Z. C. Hu, Y. G. Zheng and Y. C. Shen, *Catal. Commun.*, 2011, **16**, 133-139.
8 N. W. Wan, Z. Q. Liu, K. Huang, Z. Y. Shen, F. Xue, Y. G. Zheng and Y. C. Shen, *RSC Adv.*, 2014, **4**, 64027-64031.
9 H. S. Kim, J. H. Lee, S. Park and E. Y. Lee, *Biotechnol. Bioprocess Eng.*, 2004, **9**, 62-64.
10 W. J. Choi, E. Y. Lee, S. J. Yoon, S. T. Yang and C. Y. Choi, *J. Biosci. Bioeng.*, 1999, **88**, 339-341.

11 J. H. Woo, Y. O. Hwang, J. H. Kang, H. S. Lee, S. J. Kim and S. G. Kang, *J. Biosci. Bioeng*., 2010, **110**, 295-297.
12 M. T. Reetz, M. Bocola, L. W. Wang, J. Sanchis, A. Cronin, M. Arand, J. Y. Zou, A. Archelas, A. L. Bottalla, A. Naworyta and S. L. Mowbray, *J. Am. Chem. Soc.*, 2009, **131**, 7334-7343.
13 M. Kotik, W. Zhao, G. Lacazio and A. Archelas, *J. Mol. Catal. B Enzym*., 2013, **91**, 44-51.
14 M. H. Woo, H. S. Kim and E. Y. Lee, *J. Ind. Eng. Chem*., 2012, **18**, 384-391.
15 M. T. Reetz, C. Torre, A. Eipper, R. Lohmer, M. Hermes, B. Brunner, A. Maichele, M. Bocola, M. Arand, A. Cronin, Y. Genzel, A. Archelas and R. Furstoss, *Org. Lett*., 2004, **6**, 177-180.
16 J. H. L. Spelberg, R. Rink, A. Archelas, R. Furstoss and D. B. Janssen, *Adv. Synth. Catal.*, 2002, **344**, 980-985.
17 B. van Loo, J. Kingma, G. Heyman, A. Wittenaar, J. H. L. Spelberg, T. Sonke and D. B. Janssen, *Enzyme Microb. Technol*., 2009, **44**, 145-153.
18 M. T. Reetz and H. B. Zheng, *ChemBioChem*, 2011, **12**, 1529-1535.
19 K. L. Morley and R. J. Kazlauskas, *Trends Biotechnol*., 2005, **23**, 231-237.
20 A. Pavelka, E. Chovancova and J. Damborsky, *Nucleic Acids Res*., 2009, **37**, W376-W383.
21 J. H. Woo, J. H. Kang, S. Kang, Y. O. Hwang and S. J. Kim, *Appl. Microbiol. Biotechnol*., 2009, **82**, 873-881.
22 H. Visser, S. Vreugdenhil, J. A. M. de Bont and J. C. Verdoes, *Appl. Microbiol. Biotechnol*., 2000, **53**, 415-419.
23 X. D. Kong, Q. Ma, J. H. Zhou, B. B. Zeng and J. H. Xu, *Angew Chem. Int. Edit.*, 2014, **53**, 6641-6644.
24 B. Schiott and T. C. Bruice, *J. Am. Chem. Soc.*, 2002, **124**, 14558-14570.
25 J. Zhao, Y. Y. Chu, A. T. Li, X. Ju, X. D. Kong, J. Pan, Y. Tang and J. H. Xu, *Adv. Synth. Catal*., 2011, **353**, 1510-1518.
26 E. Y. Lee, *J. Ind. Eng. Chem*., 2007, **13**, 159-162.
27 H. X. Jin, Z. C. Hu and Y. G. Zheng, *J. Biosci.*, 2012, **37**, 695-702.
28 H. X. Jin, Z. Q. Liu, Z. C. Hu and Y. G. Zheng, *Eng. Life Sci.*, 2013, **13**, 385-392.
29 P. F. Gong and J. H. Xu, *Enzyme Microb. Technol.*, 2005, **36**, 252-257.
30 H. Baldascini, K. J. Ganzeveld, D. B. Janssen and A. A. C. M. Beenackers, *Biotechnol. Bioeng.*, 2001, **73**, 44-54.
31 Z. Q. Liu, Y. Gosser, P. J. Baker, Y. Ravee, Z. Y. Lu, G. Alemu, H. G. Li, G. L. Butterfoss, X. P. Kong, R. Gross and J. K. Montclare, *J. Am. Chem. Soc.*, 2009, **131**, 15711-15716.
32 F. Xue, Z. Q. Liu, N. W. Wan and Y. G. Zheng, *Appl. Biochem. Biotechnol*., 2014, **174**, 352-364.
33 M. Bradford, *Anal. Biochem*., 1976, **72**, 248-254.
34 U. K. Laemmli, *Nature*, 1970, **227**, 680-685.
35 F. Cedrone, T. Bhatnagar and J. C. Baratti, *Biotechnol. Lett*., 2005, **27**, 1921-1927.
36 A. Fiser and A. Sali, *Method Enzymol.*, 2003, **374**, 461-491.
37 C. Zhang, J. Li, B. Yang, F. He, S. Y. Yang, X. Q. Yu and Q. Wang, *RSC Adv.*, 2014, **4**, 27526-27531.
38 F. Osterberg, G. M. Morris, M. F. Sanner, A. J. Olson and D. S. Goodsell, *Proteins*, 2002, **46**, 34-40.